Efficient and Noise Resilient Measurements for Quantum Chemistry on Near-Term Quantum Computers: Supplementary Information

William J. Huggins,[1,2,3,∗] Jarrod R. McClean,[1] Nicholas C. Rubin,[1] Zhang Jiang,[1] Nathan Wiebe,[1,4,5] K. Birgitta Whaley,[2,3] and Ryan Babbush[1,†]

[1]*Google Quantum AI, Venice, CA 90291*
[2]*Department of Chemistry, University of California, Berkeley, CA 94720*
[3]*Berkeley Quantum Information and Computation Center,*
University of California, Berkeley, CA 94720
[4]*Pacific Northwest National Laboratory, Richland WA 99354*
[5]*Department of Physics, University of Washington, Seattle, WA 98105*

(Dated: November 20, 2020)

∗ corresponding author: whuggins@google.com

† corresponding author: ryanbabbush@gmail.com

SUPPLEMENTARY NOTE I: VARIANCE BOUNDS

In the text of the main article, we reviewed the standard approach to upper bounding the number of measurements (M) required to measure the energy of a Hamiltonian (H) to within a desired target precision ϵ [1, 2]. This bound is calculated in a straightforward way from the qubit representation that is obtained by making the Jordan-Wigner transformation on a second quantized representation of the fermionic states, by expressing H as the sum of Pauli strings (products of single-qubit Pauli operators) P_ℓ acting on the qubit representation of the state. Then we have

$$M_q \leq \left(\frac{\sum_\ell |\omega_\ell|}{\epsilon} \right)^2, \quad \text{where} \quad H = \sum_\ell \omega_\ell P_\ell. \tag{1}$$

More generally, if the Hamiltonian is expressed as a linear combination $H = \sum_\ell \omega_\ell O_\ell$, one can work out the optimal way of distributing independent measurements between these terms and the overall number of measurements required for the resulting estimator to attain a target precision. We refer the reader to Ref. 2 for more details and simply recall the expression here,

$$M = \left(\frac{\sum_\ell |\omega_\ell| \sigma_\ell}{\epsilon} \right)^2. \tag{2}$$

The notation is the same as above, except that σ_ℓ is the positive square root of the variance of the operator O_ℓ. The upper bound of Supplementary Eq. (1) is derived by noting that the variance of a Pauli operator measurement is at most one and by performing the appropriate substitutions. Our primary concern here is to show how the calculation of such a bound for fermionic Hamiltonians depends in a subtle manner on the representation of the Hamiltonian. We have denoted the bounds above M_q, to refer to their evaluation in the qubit representation of the Hamiltonian.

When calculating an upper bound of this type for a quantum chemical Hamiltonian,

$$H = \sum_{pq} h_{pq} a_p^\dagger a_q + \sum_{pqrs} h_{pqrs} a_p^\dagger a_q^\dagger a_r a_s, \tag{3}$$

it might seem natural to work directly with the coefficients h_{pq} and h_{pqrs} and the fermionic representation rather than performing the Jordan-Wigner transformation to the qubit representation. Provided that one is careful to count the coefficient for each term and its Hermitian conjugate only once, it is possible to obtain an upper bound to the number

of measurements required directly from the coefficients h_{pq} and h_{pqrs}. Provided that the Hamiltonian is normal-ordered first, this bound can be expressed as

$$M_f \leq \left(\frac{\sum_{p,q \leq p} |h_{pq}| + \sum_{pqr,s<q} |h_{pqrs}| + \sum_{pq,r \leq p,s=q} |h_{pqrs}|}{\epsilon} \right)^2. \qquad (4)$$

We denote this bound by M_f to indicate it was derived in the fermionic representation of the Hamiltonian. However, this bound is looser than necessary in multiple ways. In Supplementary Table I we show a breakdown of the calculation of the sum of the absolute values of the coefficients for the Hamiltonian of a chain of eight equally spaced hydrogen atoms. We consider five different types of terms from Supplementary Eq. (3) and calculate the sum of the absolute values of the coefficients for all terms of each type in both the qubit and fermionic representations. By comparing the two approaches in this way we show below that we can shed light on the difference in the resulting bounds.

In column I of Supplementary Table I we begin with this analysis for the 'number operator' terms, $a_p^\dagger a_p$ of partition I. We see that the value reported in the qubit representation is exactly half of that reported in the fermionic one. This is because the Jordan-Wigner transformation applied to $a_p^\dagger a_p$ yields $\frac{1}{2}\mathcal{I} + \frac{1}{2}Z_p$. However, we may neglect the first contribution since this is a constant and so does not affect the variance. Another way of understanding this difference between the qubit and fermionic contributions is to realize that the bound of Supplementary Eq. (1) is derived with the assumption that the maximum variance of each term is 1. The number operator, however, has eigenvalues 0 and 1 rather than -1 and 1 like a Pauli operator, and so its maximum variance is lower. We shall present an alternative to Supplementary Eq. (4) below in Supplementary Eq. (8) that accounts for this lower variance. The analysis of the other one-body term, $a_p^\dagger a_q + h.c.$, from partition II, is simpler. Column II shows that the part of the total magnitude of the coefficients of these terms is the same, regardless of which representation is used for the calculation.

The two-body terms in the Hamiltonian display more varied behavior. Taking a term from partition III and applying the Jordan-Wigner transformation results in exactly $\frac{1}{4}$ of the weight being assigned to a constant term, explaining the difference between the values for this partition. Because terms such as $a_p^\dagger a_q^\dagger a_p a_q$ can be rewritten as the product of two number operators, they must have eigenvalues 0 and 1 and thus, a maximum variance smaller than one. This improved bound would actually be lower than the one suggested by the analysis of the Jordan-Wigner transformed terms, because it would account for the covariances between

3

Hamiltonian Partition	I	II	III	IV	V	Whole Hamiltonian
Example Term	$a_p^\dagger a_p$	$a_p^\dagger a_q + h.c.$	$a_p^\dagger a_q^\dagger a_p a_q$	$a_p^\dagger a_q^\dagger a_q a_r + h.c.$	$a_p^\dagger a_q^\dagger a_r a_s + h.c.$	-
Fermionic $\sum_\ell |w_\ell|$	32.288	2.852	34.214	7.436	35.579	112.368
Qubit $\sum_\ell |w_\ell|$	16.144	2.852	25.660	6.794	17.790	33.500

Supplementary Table I. Consider the normal ordered second quantized quantum chemistry Hamiltonian of Supplementary Eq. (3), calculated for a chain of eight hydrogen atoms equally spaced 1.0Å apart in an STO-3G basis. We group the terms in this Hamiltonian into five partitions. Partitions I and II contain the one particle terms from the first summation. Partition I consists of those terms where $p = q$, while II consists of those where $p \neq q$. Partitions III, IV, and V contain the two particle terms from the second summation. Partition III consists of those where there are two unique values among p, q, r, and s, while IV consists of those with three unique values and V consists of those with four eigenvalues. For each partition, we report the sum of the absolute values of the coefficients of these terms in the fermionic representation of the Hamiltonian (counting the coefficient of a term and its Hermitian conjugate only once). We also report the same quantity calculated in the qubit representation after applying the Jordan-Wigner transformation. We drop any constant terms which appear as a result of the Jordan-Wigner transformation, since these do not contribute to the variance. Additionally, we report the sum of the absolute value of the coefficients for the entire Hamiltonian calculated in both ways in the final column.

the Z_p, Z_q, and $Z_p Z_q$ terms that emerge. We shall incorporate this tighter bound on the variance of the individual terms in this class into the alternative to Supplementary Eq. (4) presented below as Supplementary Eq. (8).

The disparity for partitions IV and V has a different source. If one performs the Jordan-Wigner transformation of a term from either class individually, there is no difference between the total magnitudes of the coefficients for the fermionic operators and their qubit counterparts. However, when one sums all such terms together there is some cancellation between the qubit terms that reduces the overall total magnitude. Specifically, the terms in class V benefit from some cancellation due to the eight-fold symmetries of the two-electron integral

tensor for real orbitals [3],

$$h_{pqrs} = h_{qpsr} = h_{rspq} = h_{srqp} = h_{rqps} = h_{qrsp} = h_{psrq} = h_{spqr} = h. \quad (5)$$

We claim that the cancellations between symmetric terms result in a value for the sum of the magnitudes of the coefficients that is exactly half as large in the qubit representation as it is in the fermionic one. As an example, consider the case with $p = 4, q = 2, r = 3, s = 1$. After normal-ordering, the eight terms become four and we have

$$2h a_4^\dagger a_2^\dagger a_3 a_1 + h.c. + 2h a_3^\dagger a_2^\dagger a_4 a_1 + h.c., \quad (6)$$

where h is given by Supplementary Eq. (5) and denotes the value of the coefficients before normal-ordering. The Jordan-Wigner transformation leads to terms from $a_4^\dagger a_2^\dagger a_3 a_1 + h.c.$ that cancel with terms from $a_3^\dagger a_2^\dagger a_4 a_1$ as shown below:

$$\frac{-h}{4}(X_1 X_2 X_3 X_4 + X_1 X_2 Y_3 Y_4 - X_1 Y_2 X_3 Y_4 + X_1 Y_2 Y_3 X_4 + Y_1 X_2 X_3 Y_4 - Y_1 X_2 Y_3 X_4 + Y_1 Y_2 X_3 X_4 + Y_1 Y_2 Y_3 Y_4) +$$
$$\frac{-h}{4}(X_1 X_2 X_3 X_4 + X_1 X_2 Y_3 Y_4 + X_1 Y_2 X_3 Y_4 - X_1 Y_2 Y_3 X_4 - Y_1 X_2 X_3 Y_4 + Y_1 X_2 Y_3 X_4 + Y_1 Y_2 X_3 X_4 + Y_1 Y_2 Y_3 Y_4) = \quad (7)$$
$$\frac{-h}{4}(X_1 X_2 X_3 X_4 + X_1 X_2 Y_3 Y_4 + Y_1 Y_2 X_3 X_4 + Y_1 Y_2 Y_3 Y_4 + X_1 X_2 X_3 X_4 + X_1 X_2 Y_3 Y_4 + Y_1 Y_2 X_3 X_4 + Y_1 Y_2 Y_3 Y_4).$$

It is straightforward, although tedious, to prove that the same cancellation occurs generically for terms in class V as a consequence of this eight-fold symmetry. As a result, for this class of terms the sum of the magnitudes of the coefficients is exactly half as large in the qubit representation as it is in the fermionic one. Analogous cancellations in the sum of the class IV terms do not show an obvious symmetry but they are also the source of the difference between the contributions from the two representations in partition IV.

Further cancellation is also apparent when one combines all five classes and calculates the sum of the absolute values of the coefficients (dropping the constant terms) for both representations of the Hamiltonian. The sum of magnitudes of the individual classes in the fermionic representation is the same as the magnitude of the sum. However, in the qubit representation, this value calculated for the entire Hamiltonian is roughly half the size of the sum of the individual partitions. One substantial reason for this difference is the fact that the terms in partitions I and III naturally give rise to terms proportional to products of single qubit Z operators having opposite signs. This is behavior that we should expect for any molecular Hamiltonian, where the single number operator terms arise from the Coulomb attraction between nuclei and individual electrons (negative sign), while the terms containing two number operators arise from the Coulomb repulsion between pairs of

electrons (positive sign). Furthermore, unlike the tighter bounds achievable by accounting for the smaller variance of the terms in partitions I and III, this cancellation derives from the underlying form of the Hamiltonian and can not be accounted for in a straightforward way by using a better upper bound for the σ_ℓ values in Supplementary Eq. (2) when deriving a fermionic bound like Supplementary Eq. (4).

In the first three rows of Supplementary Table II, we now tabulate the bounds on the variance of the energy estimator, in units of $100\ E_h^2$, that arise from the sums of the absolute values of the coefficients. We perform these calculations for a chain of eight hydrogen atoms at various symmetric stretched interatomic spacings, including the 1.0Å distance explored in Supplementary Table I. In this table, 'Qubit Variance Bound' refers to the bound of Supplementary Eq. (1) calculated using the qubit form of the Hamiltonian. 'Naive Fermionic Variance Bound' is calculated in a similar way, except using the sums of the fermionic coefficients, as in Supplementary Eq. (4). As noted above, the terms in the Fermionic Hamiltonian which consist of number operators (class I in Supplementary Table I) or products of number operators (class II in Supplementary Table I) actually have a variance which is upper-bounded by $\frac{1}{4}$ rather than one. One can substitute this tighter bound in Supplementary Eq. (2) to yield the expression

$$M_f \leq \left(\frac{\frac{1}{2}\sum_p |h_p| + \sum_{p,q<p} |h_{pq}| + \sum_{pqr,s<q} |h_{pqrs}| + \sum_{pq,r<p,q} |h_{pqrq}| + \frac{1}{2}\sum_{pq} |h_{pqpq}|}{\epsilon} \right)^2,$$

(8)

where we have assumed that the Hamiltonian is normal-ordered to simplify the expression. We present calculation based on this improved bound in the row titled 'Fermionic Variance Bound.' However, it is clear that the bounds obtained directly from the qubit representation of the Hamiltonian are considerably tighter than either of the bounds obtained using the fermionic representation. This difference is explained by the cancellation effects that we have described above.

In addition to these bounds on the variance of the estimator for the Hamiltonian, we also consider two approximations to this variance that are not guaranteed to be upper bounds (rows 4 and 5 of Table II). These approximations, which we refer to for brevity as FVA and QVA, are calculated using the methodology of Ref. 1 using the fermionic and qubit Hamiltonians respectively. In that work Wecker et al. reasoned that, in a typical quantum chemical calculation, the orbitals would have occupation numbers near 0 or 1. Therefore,

6

Interatomic Spacing (Angstrom)	.6	.7	.8	.9	1.0	1.1	1.2	1.3
Qubit Variance Bound	22.499	17.657	14.680	12.675	11.222	10.134	9.297	8.629
Fermionic Variance Bound	99.393	86.271	76.352	68.683	62.596	57.721	53.768	50.462
Naive Fermionic Variance Bound	205.251	177.997	156.704	139.847	126.267	115.234	106.168	98.545
Fermionic Variance Approximation	31.501	27.404	24.580	22.557	21.038	19.893	19.023	18.321
Qubit Variance Approximation	7.212	6.225	5.567	5.118	4.786	4.540	4.356	4.209
Hartree-Fock Variance	7.211	6.224	5.565	5.118	4.785	4.539	4.355	4.208
Ground State Variance	9.206	8.194	7.568	7.181	6.929	6.779	6.695	6.641

Supplementary Table II. Variances for a symmetrically stretched chain of 8 hydrogen atoms in an STO-3G basis. Rows 1-5 show values of the variance bounds and approximations to these that are described in the text. The variances are presented in units of 100 E_h^2. The bound in row 1 is calculated using Supplementary Eq. (1), while row 2 uses Supplementary Eq. (8), and row 3 uses Supplementary Eq. (4). The approximations in rows 4-5 are calculated using the methodology of Ref. 1, which amounts to using Supplementary Eq. (1) or Supplementary Eq. (4) but neglecting some of the terms in the Hamiltonian as described in the text below. The last two rows, 6-7, present the actual variance of an estimator that measures each term in the Jordan-Wigner transformed Hamiltonian separately, for the Hartree-Fock state and for the ground state, respectively.

the number and number-number terms in the Hamiltonian (partition I and partition III in Supplementary Table I) would have a variance that is close to zero. This assumption is satisfied exactly for the Hartree-Fock state when the appropriate single-particle basis is used, and should be approximately true when Hartree-Fock is qualitatively correct. Based on this assumption, Ref. 1 neglected these terms and then approximated the variance of the remaining terms in the Hamiltonian using the type of bounds we have already discussed.

Rows 4 and 5 of Table II show that that there is still a substantial difference between the variances calculated under this approximation using the two different representations of the Hamiltonian, i.e., between FVA and QVA. This is primarily due to the reduction caused by the cancellations among the double-excitation terms (class V in Supplementary Table I). Interestingly, the numbers presented for the 'Qubit Variance Approximation' (QVA) are nearly identical to those for the actual variance expected when measuring the Hartree-Fock

state (row 6). In fact, any differences between these values are found to arise purely from numerical precision issues in the data. One can examine the Pauli operators that arise from performing the Jordan-Wigner transformation on the Hamiltonian after deleting the diagonal terms and see that each of them has an expectation value of exactly zero on the Hartree-Fock state. Measurements of these terms therefore achieve the maximum possible variance of 1, while measurements of the deleted diagonal terms would have a variance that is exactly 0. Thus, the calculation of the actual variance (when measuring each term in the Hamiltonian separately) using Supplementary Eq. (2) for the Hartree-Fock state then yields the same value as the calculation of the bound of Supplementary Eq. (1) under the approximation proposed by Ref. 1.

SUPPLEMENTARY NOTE II: APPLYING THE FERMIONIC RDM CONSTRAINTS TO THE QUBIT HAMILTONIAN

In the previous section we saw a substantial difference between the bounds calculated from the fermionic operators and those calculated from the qubit operators after applying the Jordan-Wigner transformation. In light of this, it is natural to ask how the reduced density matrix (RDM) approach of Ref. 2 might perform when formulated using the qubit representation of the Hamiltonian. In Ref, [2], Rubin et al. proposed that one could use known n-representability constraints on the expectation values of few-fermion operators, in order to construct estimators for the expectation value of the Hamiltonian that will have lower variance. They showed how one could take a collection of algebraic equalities from these fermionic n-representability constraints and use them to construct a new Hamiltonian $\tilde{H}$ from the original H. According to their approach, $\tilde{H}$ is constructed to have the same expectation value as H, but a lower maximum variance according to the bounds discussed above. They performed this minimization of the upper bound using standard linear programming techniques.

We are primarily focused here on the impact of these techniques for a real-world experiment. Therefore, we shall compare the impact of performing this minimization on the fermionic and qubit representations of the Hamiltonian, using the actual observed variance with respect to the ground state as the figure of merit, rather than employing the bounds or approximations discussed above. We take the same Pauli Word Grouping strategy described
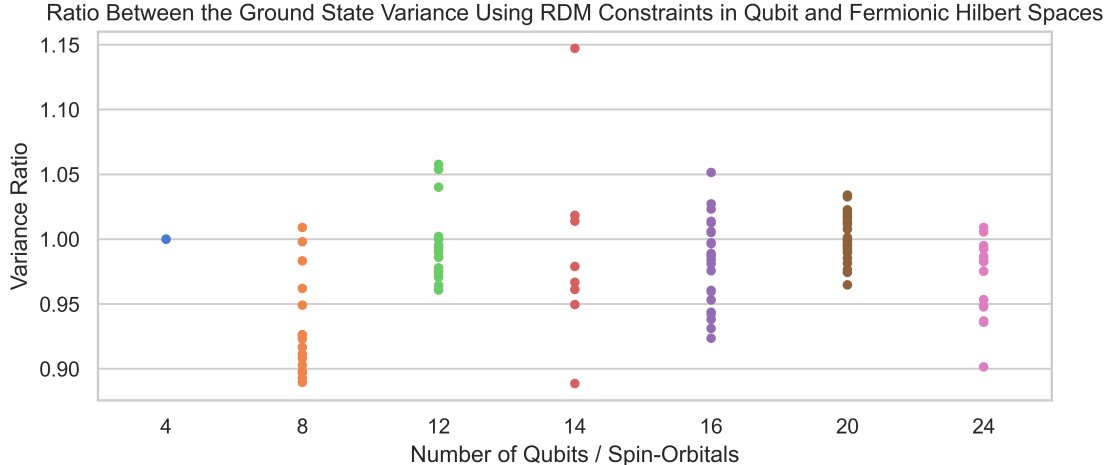
Supplementary Figure 1. For each of the systems considered in the main text we apply the techniques of Ref. 2 to the Hamiltonians in the fermionic and qubit Hibert spaces. We list these systems in Supplementary Table III below, duplicating Table II of the main text for convenience. Using fermionic n-representability constraints, we construct the Hamiltonians $\tilde{H}_{fermionic}$ and $\tilde{H}_{qubit}$, that have the same expectation value but a lower maximum variance under bounds of the type described by Supplementary Eq. (1) and Supplementary Eq. (4). We then consider the variance of these Hamiltonians with respect to the ground state. We calculate these variances assuming measurement is performed using the Pauli Word Grouping strategy described in the main text. Finally, we plot the ratio of the variance obtained for $\tilde{H}_{qubit}$ with the variance obtained for $\tilde{H}_{fermionic}$. The fact that all of these ratios are found to be near 1 shows that reformulating the work of Ref. 2 in the qubit representation does not offer a substantial improvement.

in the main text and apply it to the Hamiltonians $\tilde{H}_{fermionic}$ and $\tilde{H}_{qubit}$. We define $\tilde{H}_{fermionic}$ and $\tilde{H}_{qubit}$ as the Hamiltonians that result from performing the upper bound minimization procedure of Ref. 2 in the fermionic and qubit representations respectively.

In Supplementary Figure 1 we plot the ratio between the variances of $\tilde{H}_{qubit}$ and $\tilde{H}_{fermionic}$ for the ground state of each of the systems considered in the main text of this work. We list these systems in Supplementary Table III below, duplicating Table II of the main text for convenience. Despite the substantial differences in the variance bounds formulated in the two representations, the impact of applying the RDM constraints to the qubit Hamiltonian rather than the fermionic one is found to be marginal, at best. For the majority of the systems it appears that the qubit-based bounds perform slightly better, but there are also

9

a number of cases where this pattern is reversed.

SUPPLEMENTARY NOTE III: LOW RANK DECOMPOSITION

In the main text, we explained that our strategy for measurement is based on rewriting the standard quantum chemical Hamiltonian in the following form:

$$H = U_0 \left(\sum_p g_p n_p \right) U_0^\dagger + \sum_{\ell=1}^L U_\ell \left(\sum_{pq} g_{pq}^{(\ell)} n_p n_q \right) U_\ell^\dagger, \tag{9}$$

where the values g_p and $g_{pq}^{(\ell)}$ are scalars, $n_p = a_p^\dagger a_p$, and the U_ℓ are unitary operators which implement a single particle change of orbital basis. Here we shall explain how one obtains that factorization starting from a standard representation. We follow the presentation of Berry et al. with minor deviations and refer the reader to Ref. 4 for more details.

First, it is necessary to obtain the Hamiltonian in the chemist's standard form,

$$H = \sum_{\sigma \in \{\uparrow, \downarrow\}} \sum_{pq} T_{pq} a_{p,\sigma}^\dagger a_{q,\sigma} + \frac{1}{2} \sum_{\alpha, \beta \in \{\uparrow, \downarrow\}} \sum_{pqrs} V_{pqrs} a_{p,\alpha}^\dagger a_{q,\alpha} a_{r,\beta}^\dagger a_{s,\beta}. \tag{10}$$

This differs from the physicist's convention of Supplementary Eq. (3), where the operators in the two-electron component of the Hamiltonian have both creation operators to the left of both annihilation operators. We assume the use of purely real spatial orbitals, and therefore the tensor V_{pqrs} inherits the eight-fold symmetry,

$$V_{pqrs} = V_{srqp} = V_{psqr} = V_{qprs} = V_{qpsr} = V_{rsqp} = V_{rspq} = V_{srpq}, \tag{11}$$

from the definition of the two-electron integrals [3].

Now we can perform the decomposition. We treat the tensor V as a matrix indexed by the collective indices pq and rs. We can eigendecompose this matrix to yield

$$V_{pqrs} = \sum_\ell w_\ell v_{pq}^{(\ell)} v_{rs}^{(\ell)} \tag{12}$$

In the above equation, w_ℓ are the eigenvalues of V, $v^{(\ell)}$ are the eigenvalues. We proceed by using this equality to rewrite the two-electron component of the Hamiltonian,

$$\frac{1}{2} \sum_{\alpha, \beta \in \{\uparrow, \downarrow\}} \sum_{pqrs} V_{pqrs} a_{p,\alpha}^\dagger a_{q,\alpha} a_{r,\beta}^\dagger a_{s,\beta} = \frac{1}{2} \sum_\ell w_\ell \left(\sum_{\sigma \in \{\uparrow, \downarrow\}} \sum_{pq} v_{pq}^{(\ell)} a_{p,\sigma}^\dagger a_{q,\sigma} \right)^2, \tag{13}$$

10

with $v_{pq}^{(\ell)}$ inheriting the symmetry between the p and q indices from V.

The final remaining step is to transform Supplementary Eq. (13), as well as the one-electron component of the Hamiltonian by diagonalizing each of the one-body operators. It is straightforward to express each of the one-body operators as diagonal operators in a rotated single-particle basis. The appropriate change of basis matrices can be obtained from the eigenvalues of the coefficient tensors, T and the $g^{(\ell)}$s in our case. We can therefore express the Hamiltonian in the form of Supplementary Eq. (9), dropping the spin indices for simplicity. The coefficients g_p come from rotating to a basis where T_{pq} is diagonal. The coefficients $g_{pq}^{(\ell)}$ likewise come from rotating to a series of bases where the tensors v^ℓ are diagonal between their p and q indices. The operators U_ℓ are the inverse of the operators that diagonalize the one-body operators $\sum_{\sigma \in \{\uparrow,\downarrow\}} \sum_{pq} T_{pq} a_{p,\sigma}^\dagger a_{q,\sigma}$ and $\sum_{\sigma \in \{\uparrow,\downarrow\}} \sum_{pq} v_{pq}^{(\ell)} a_{p,\sigma}^\dagger a_{q,\sigma}$. Note that the p and q indices of Supplementary Eq. (9) represent new dummy indices and that the w_ℓ terms have been absorbed into $g_{pq}^{(\ell)}$, together with the contributions from the squares of the diagonalized v_{pq}^ℓ terms.

SUPPLEMENTARY NOTE IV: DESCRIPTION OF DATA

In addition to this supplementary text, we also include the raw data we have generated through our numerical calculations which does not already appear in tables throughout the manuscript. The data is provided as a table in the csv file format with each row corresponding to one of the particular systems listed below in Supplementary Table III (identical to Table II in the main text) and each column corresponding to the variance of a different estimator (or an ancillary piece of data, such as the energy of the system). Energies are provided in units of E_h and variances in units of E_h^2.

[1] Wecker, D., Hastings, M. B. & Troyer, M. Progress towards practical quantum variational algorithms. *Phys. Rev. A* **92**, 042303 (2015). URL https://journals.aps.org/pra/abstract/10.1103/PhysRevA.92.042303.

[2] Rubin, N. C., Babbush, R. & McClean, J. Application of fermionic marginal constraints to hybrid quantum algorithms. *New J. Phys.* **20**, 053020 (2018). URL https://iopscience.iop.org/article/10.1088/1367-2630/aab919/meta.

System	Interatomic Spacings (Å)	Basis Set	Total Orbitals	Frozen Orbitals	Number of Qubits
H_2	.6, .7, ... 1.3	STO-3G	2	None	4
H_2	.6, .7, ... 1.3	6-31G	4	None	8
H_4	.6, .7, ... 1.3	STO-3G	4	None	8
H_6	.6, .7, ... 1.3	STO-3G	6	None	12
H_4	.6, .7, ... 1.3	6-31G	8	None	16
H_8	.6, .7, ... 1.3	STO-3G	8	None	16
H_2	.6, .7, ... 1.3	cc-pVDZ	10	None	20
H_{10}	.6, .7, ... 1.3	STO-3G	10	None	20
H_6	.6, .7, ... 1.3	6-31G	12	None	24
H_2O	.8, .9, ... 1.5	STO-3G	7	1	12
H_2O	.8, .9, ... 1.5	STO-3G	7	None	14
H_2O	.8, .9, ... 1.5	6-31G	13	1	24
N_2	.9, 1.0, ... 1.6	STO-3G	10	2	16
N_2	.9, 1.0, ... 1.6	STO-3G	10	None	20

Supplementary Table III. List of the molecular systems considered in this work, displayed in order of increasing number of qubits, for each type of system. This is a duplicate of Table II in the main text, with an additional column indicating the total number of spatial orbitals. The hydrogen chain systems (H_n) are all arranged in a line, with equal interatomic spacing. The interatomic spacing for the water molecules (H_2O) refers to the length of the symmetrically stretched O-H bonds, which are separated by a fixed angle of 104.5 deg. Total Orbitals refers to the number of spatial molecular orbitals used for each system. A non-zero number of frozen orbitals indicates the number of molecular orbitals fixed in a totally occupied state.

[3] Szabo, A. & Ostlund, N. S. *Modern Quantum Chemistry: Introduction to Advanced Electronic Structure Theory* (Courier Corporation, 2012). URL `https://play.google.com/store/books/details?id=KQ3DAgAAQBAJ`.

[4] Berry, D. W., Gidney, C., Motta, M., McClean, J. R. & Babbush, R. Qubitization of arbitrary basis quantum chemistry leveraging sparsity and low rank factorization. *Quantum* **3**, 208 (2019). URL `https://arxiv.org/pdf/1902.02134.pdf`.